East European Journal of Physics. **2.** 267-276 (2023)
DOI:10.26565/2312-4334-2023-2-30 ISSN 2312-4334

EXPERIMENTAL SIMULATION FOR TWO OPTICALLY FILTERED MODULATION WEIGHTS IN LASER DIODE AS A SELF-LEARNING LAYER†

Dhuha Raad Madhloom[a]*, Ayser A. Hemed[b]†, Suha Musa Khorsheed[a]‡
[a]*Department of Physics, College of Science, University of Al-Nahrain, Baghdad, Iraq*
[b]*Department of Physics, College of Education, Mustansiriyah University, Baghdad, Iraq*
**Corresponding author's e-mail: duha.raad23@gmail.com*
†*E-mail: ayser.hemed@uomustansiriyah.edu.iq*
‡*E-mail: suhaalawsi@gmail.com*
Received March 25, 2023; revised April 17, 2023; accepted April 19, 2023

In this study, the response of a nonlinear laser medium is experimentally studied. In the study, a hybrid version of the input layer that multiplies optically and accumulates electrically is compared with a wholly optical version that multiplies and accumulates optically. This medium is subjected to two different paths of optically filtered and attenuated feedback. With such a system, the variation of feedback weight in one of them is tested in correspondence to the second one. Observations for frequency spectra are carried out to simulate the resultant response with an input layer for a neural network based on chaotic carriers. Chaotic laser emission was observed as a function of several control parameters, which are D.C. bias voltage, branch optical attenuation, and feedback strengths based on filtration with fiber Bragg grating. This learning rule is linear in the difference between each input and output of a neuron. This is an enhancing/inhibiting rule. The thresholds are adjusted in such a way that the output of the neuron is either pushed in the same direction as the input (enhancing) or pushed in the opposite direction (inhibiting).
Keywords: *Machine Learning; Neural Network; Chaotic Modulation; Laser Diode; Light Brain*
PACS: 42.55.Wd, 42.65.Sf, 42.79.Hp, 42.79.Sz, 85.60._q

1. INTRODUCTION

Optical neural network development initially described the fundamentals of an optical matrix multiplier for linear operation based on the theory of artificial neural networks. The optical neural network created by waveguide optical interconnection and free-space optical interconnection is then introduced. Finally, we discuss optical neural networks' nonlinearity [1]. Both connection topologies and the response dynamics of individual neurons influence computations in biological brain networks. The Hodgkin-Huxley framework is the foundation for a broad and biologically plausible family of computational models for single neurons known as conductance-based neuron models. These nonlinear dynamical systems relate the ionic current flow into and out of the neuron to the temporal evolution of the voltage across the neuronal membrane. Instead of simulating a binary-valued train of spike events, they model the continuous-valued membrane voltage, which allows them to generate a diverse range of neuronal activities, such as subthreshold oscillations, spikes, and bursts of different waveforms. In addition, by appropriately simplifying the underlying dynamical system, their complexity may frequently be tailored to the particular situation at hand [2].

Machine learning, which includes deep learning, is a subset of the larger area of artificial intelligence. With its billions of interconnected neurons serving as processing units, the deep architecture of the human brain is the model that deep learning attempts to mimic. Our brains likewise function hierarchically, beginning with more basic thoughts and building upon them to understand more sophisticated notions. Deep learning models, which divide incoming data into features and then recombine them to complete the job at hand, reflect this way of learning (e.g., detection, classification). A deep learning model can be used to do tasks of a similar nature without human input once it has acquired important features during the training phase [3]. Early in the 1980s, optical neural networks had already been created. These systems were able to recognize faces, learn Boolean operations, and decode handwriting. Optical networks take advantage of any optical device's benefits over electrical ones, such as their capacity to transport data from a single point source to any number of recipients, whereas doing so with electronics would require a lot of cable volume. Compared to electrical systems, optical systems produce less heat. Yet, the bulk and lack of scalability of all these optical solutions are common flaws [4].

The current state of the system, $x(t)$ and the state of the system at a previous time point, $x(t-\tau)$, are frequently used to predict the temporal evolution of physical, biological, and technological systems. The output optical frequency modes of a laser are determined by the time it takes for light to complete one round-trip of the resonant cavity. Time delays are crucial to the mechanisms governing the formation of white blood cells and breathing rate in the human physiological system. Electronic and fiber-optic cable time delays are frequently assessed and taken into account in modern communication systems. The interaction of delay τ established by attenuation element and nonlinearity existing in the laser active medium $F(x) = \{x(t), x(t-\tau)\}$ in such systems can generate a rich array of chaotic dynamical effects that are sometimes intrinsic for maintaining proper operation and other times detrimental.

† ***Cite as:*** D.R. Madhloom, A.A. Hemed, and S.M. Khorsheed, East Eur. J. Phys. **2**, 267 (2023), https://doi.org/10.26565/2312-4334-2023-2-30

2. THEORETICAL CONCEPTS

A neural network is a system with inputs and outputs that consists of numerous straightforward processing components that are similar in nature. Each of the processing elements has several internal variables called "weights". The behavior of an element will change if its weights are changed, and the entire network's behavior will change as a result [5]. In 1943, Walter Pitts [6] developed the first artificial neural network (ANN) model based on arithmetic and algorithms that mimicked the principles and functions of biological nerve cells. This model was successful in performing logical operations, ushering in the era of ANNs [7]. A decades-old artificial intelligence method involves simulating brain neurons to develop sophisticated machine learning models. This method has produced both remarkable advancements and disappointing results. Because of tremendous advances in mathematical formulations and computational capacity, we can now build many more layers of virtual neurons than at any other time in the history of science [8]. By utilizing technology based on free space and an integrated platform, optical neural networks are able to process information in parallel. In this section, we'll discuss optical computing and how to design neural networks using optical techniques. Refers to an optical neural network (ONN), which has numerous linear layers connected in a convoluted manner. Due to optical interconnection's high degree of parallelism, the beam's ability to transverse the room without interfering with it, and the speed at which light propagates, time delay, and dispersion are essentially nonexistent [9]. Individual neurons in biological networks are stimulated by external currents, if any, as well as by currents received from other neurons that are presynaptic to them. DDF neurons are useful as effective network nodes in computational models of functional neural networks because the presynaptic voltage and the postsynaptic voltages describe the gap junction and synaptic current connections [10].

In terms of intensity, phase, and carrier dynamics, optical feedback in LDs can result in extensive nonlinear behavior [11]. The full scenario calls for reviewing laser dynamics with modulation for the communications application and researching the effects of direct modulation on laser rate equations. Let the laser bias componentI_b, the sinusoidal component of wave amplitude I_m, then the modulation frequency f_m are combined to provide the injection current $I(t)$ [12] [13];

$$I(t) = I_b + I_m \sin(2\pi f_m t) \tag{1}$$

Chaotic behavior in semiconductor laser is well understood, where these lasers' peak output power varies in an unpredictable manner [14]. The possible application of chaotic encryption-based cryptography makes chaotic behavior in LDs important and with direct current modulation can be represented by the following rate equations for the photon density P, carrier density N, and the driving current I as follows [15]:

$$\frac{dN}{dt} = \frac{1}{\tau_e}\left[\frac{I_b + I_m \sin(\emptyset)}{I_{th}} - N - \frac{N-\delta}{1-\delta}P\right] \tag{2}$$

The modulation is not for the complex field but for the carrier density through the disturbance to the injection current, therefore using the rate equation of the photon number P and can be written below take the form [16]:

$$\frac{dP}{dt} = GP + R_{sp} - \frac{P}{\tau p} \tag{3}$$

$$\frac{dN}{dt} = \frac{I}{q} - \frac{N}{\tau c} - Gp \tag{4}$$

where the number of electrons N, change with time inside the active region.

For a single-mode laser $G = \Gamma Vg\, \mathcal{G}m = G\,N(N - N_0)$, G is the net rate of stimulated emission and R_{sp} is the rate of spontaneous emission in to the lasing mode. Phase modulation can be included through the equation [16]:

$$\frac{d\varphi}{dt} = \frac{1}{2}\beta_c\left[GN(N - N_0) - \frac{1}{\tau p}\right] \tag{4}$$

where β_c is the amplitude-phase coupling parameter, commonly called the line width enhancement factor.

Circuit roles in the dynamics of OEF are played by the feedback delay time and feedback ratio [17]. There are two forms of OEF, the first of which is positive and the second of which is negative. In both circumstances, we can anticipate that the laser output power will exhibit regular pulsing, quasi-periodic pulsing, and chaotic pulsing states [18]. Only negative OEF is seen in the real experimental system; the region of the frequency-locked state is relatively small for positive OEF. The self-OEF system is one of the chaotic OEF with wave length filter systems proposed in LDs.

Many types of optical filter are using absorbing glass filter, color filter tunable filter, band pass filter, Notch filter, Edge filter, Fabry-Perot filter [19] and fiber Bragg grating filter [20]. Additional types are infrared filter, absorptive filter, ultraviolet filter, and Dichroic filter [21].

The processing element used in the layer simulation in this paper, is corresponding to minor Adaline [5], which is shown in Fig. 1. It has an input vector $X = \{x_i\}$, which contains n (=2) components subtracted from unique laser, and a single output y from itself, and a weight vector $W=\{w_i\}$, which also contains n (=2) components. The weights are variable (two different Bragg wavelengths) coefficients indicated by circles with arrows. The output y equals the sum of inputs multiplied by the weights and then passed through a nonlinear function. When Adalines are connected together, the layer

will become feed-forward neural network. The optimization of a posterior distribution over the states at all time points and the unknown parameters might be used as an alternative to filtering methods. In addition to finding nonlinear parameters in nonlinear and even chaotic models, optimization-based techniques have been successfully employed to estimate linear parameters in neural networks [10].

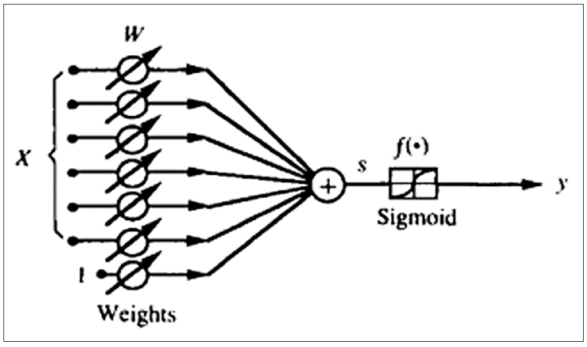

Figure 1. Adaline with sigmoid [5] [3].

Experimental Set-up

As shown in Figure 2(a), the experimental set-up includes a laser source; its model is HFCT5205A, which is a laser diode with an operational wavelength of 1310 nm and a maximum measured power of 0.048 mV at 25.5°C.

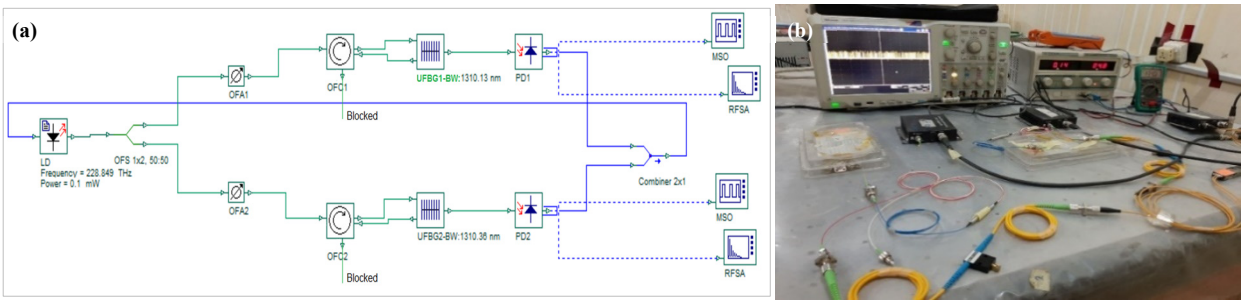

Figure 2. Experimental set-up for two branches filtered and attenuated optoelectronic feedback.

The light emitted from this source is divided into two parts via an optical fiber splitter (OFS); the first one is directed toward a first optical fiber attenuator (OFA1), then to a first fiber optical circulator (OFC1), with a blocked reflected port, and then enters a uniform fiber Bragg grating (UFBG1) with its fiber type SMF-28E, reflectivity 84%, and a Bragg wavelength (λ_B) equal to 1310.13 nm. The transmission or UFBG exit is connected with a first photodetector (PD1), whose model is BT-1VE-T, which gives the radio frequency (RF) signal to a mixed storage oscilloscope (MSO) and RF spectrum analyzer. The detect signal is also directed toward the laser bias to mix with its DC bias and then upload selected portions to the laser source. The same scenario is followed with the second output port signal that emerges from the OFS, passing through a second (OFA2), a third (UFBG2), and a fourth (PD2), then finally being added to the laser bias with selected portions. The UFBG2 has a fiber type of SMF-28E, a reflectivity of 83%, and a Bragg wavelength (λ_B) equal to 1310.36 nm. As a result, the laser is subject to selected amounts of opto-electronic feedback (OEF), which originated from itself but passed through two different optical paths. BW is λ_B, remaining abbreviations are given during the text. The figure is drawn by the Optisystem program only for clarity. Photographic picture for selected active run during the experiment operation based on Figure (2, b).

3. RESULTS AND DISCUSSIONS

Based on the configuration given in Figure 1, the laser is subjected to filtered optoelectronic feedback from two different narrow filters, with slightly different. This situation gives the facility for studying the weight of each feedback branch separately, even if both are returned to add to each other's. The laser responds nonlinearly to these feedbacks via optoelectronic feedback. Such a response can give a simulation idea inside the laboratory about the behaviors of nonlinear components in biological cells included in the brain. With such interactions, the communication system is of the electrochemical type. The focus of statistical inference has frequently been on monitoring dynamical variables, like membrane voltage, over time. The results are classified mainly according to optoelectronic feedback level, as shown in Table 1. In which, the measured parameters are the optical powers that flow after attenuation variation plus the laser bias current that resulted after tuning the observed time series by the MSO to recognize the shape of this signal from any side noise that may have been collected due to unwanted effects. The table's last two right columns, which represent the weighted feedback ratio with respect to the two branches, are summarized in the plot numbered with Figure 3.

Table 1. Experimentally measured parameters classified according to feedback strengths

No.	LD measured current (mA)	Measured power after OFA1 (uW)	Measured power after OFA2 (uW)	(OFA1-OFA2) /OFA1	(OFA2-OFA1) /OFA2
1	132.2	1.79	0	100.00%	-
2	131.1	1.79	56.7	-3067.60%	96.84%
3	129.5	27.8	2.5	91.01%	-1012.00%
4	129.5	33.6	6.5	80.65%	-416.92%
5	129.5	42.0	12.1	71.19%	-247.11%
6	129.9	57.02	32.8	42.48%	-73.84%
7	126	57.2	51	10.84%	-12.16%
8	131	67.5	158	-134.07%	57.28%
9	132	64.3	69.2	-7.62%	7.08%
10	130	63.4	8	87.38%	-692.50%
11	133	38.4	69.7	-81.51%	44.91%

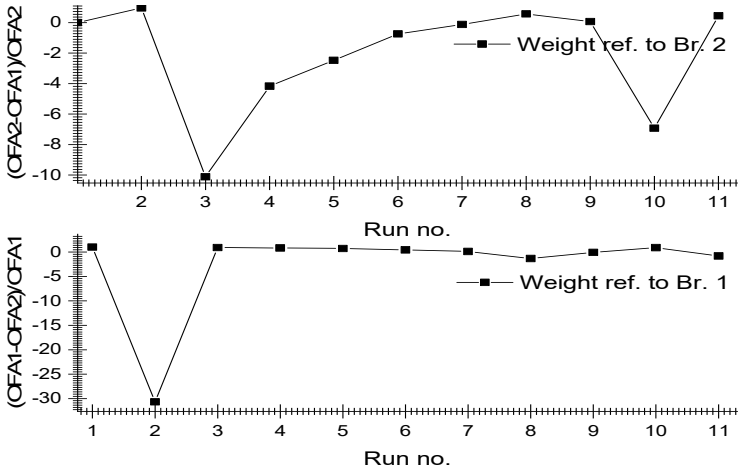

Figure 3. Summery for weighted optical feedback ratios before filtering and detection.

The first step is evaluating the weight of branch one; thus, our selection for operating is investigated with only one feedback branch, where the power is vanished in the second branch, and results show the spectra given in Figure 4.

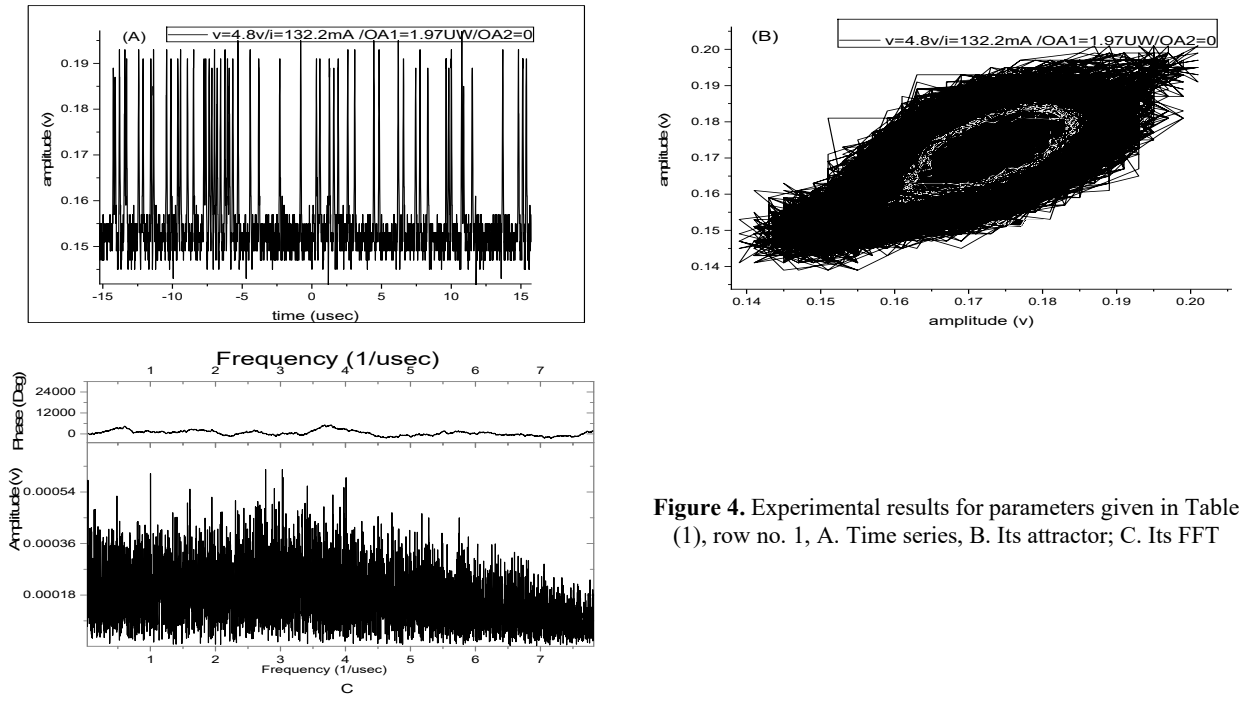

Figure 4. Experimental results for parameters given in Table (1), row no. 1, A. Time series, B. Its attractor; C. Its FFT

Observed time series, uSec scaled, in this figure shows period one and period two emission with a broad and extended limit circle attractor, while the frequency spectrum shows complete chaotic emission with around 7 MHz of

extended spectrum. This observation indicates and reinforces the assumption for the single branch weight in this experiment, where the laser is responding chaotically to its filtered feedback. This result is identical to the operation in single scaled attenuated optoelectronic feedback given in [22], but the difference is located in the feedback ratio after filtering, which is not recorded in that article, i.e., the border frequency spectrum is the result of this observation.

Introducing the second feedback branch contribution, with zero attenuation, affected the resulted spectrum directly; this is observable easily in Figure 5 via the phase and frequency spaces, furthermore time series. Phase space has turned into a fully contiguous area, indicating a huge number of newly generated chaotic modes. The frequency spectrum has a higher amplitude value, roughly twice that in Figure 4, and the overall shape of the signal is identical to a Gaussian curve with 13 MHz extended compared with less in the last-mentioned figure. This observation indicates the weight and contribution of the second feedback branch in the laser, as a nonlinear medium, resulting in dynamics.

Switching the feedback strengths ratio to roughly the same as that given in Figure (5), 91.01% reference to branch one, between the branches leads to different effects on the signal combination entering the laser medium, this being off course due to the difference in filter width that comes from it each branch weight or strength.

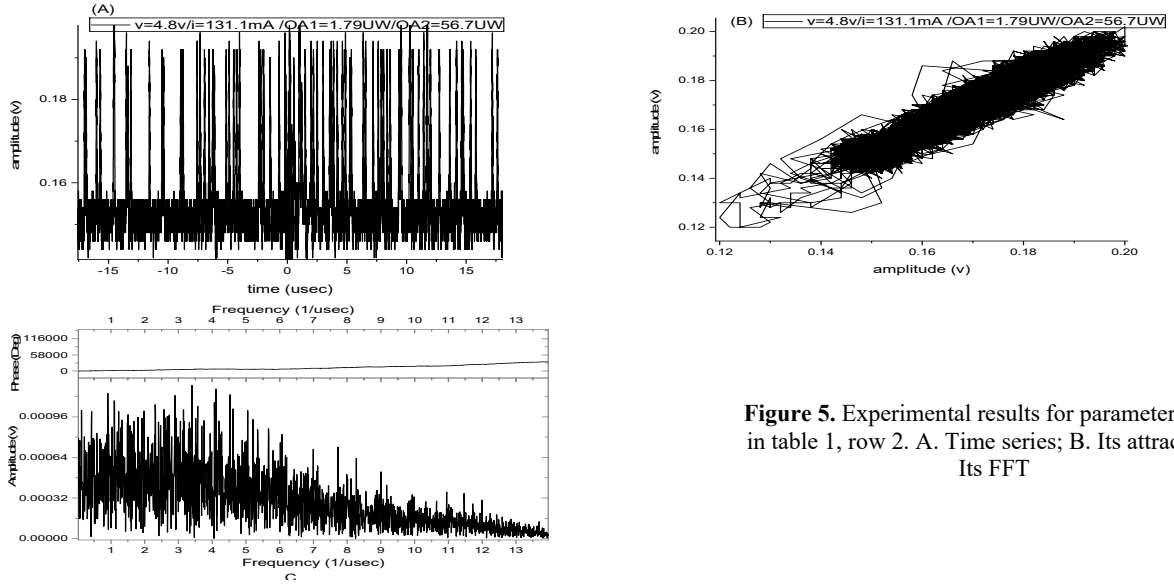

Figure 5. Experimental results for parameters given in table 1, row 2. A. Time series; B. Its attractor; C. Its FFT

As shown in Figure 6, time scale is developed to 2 uSec, and the frequency width for the chaotic signal is also extended to be 130 MHz with a higher amplitude signal, and the attractor having more smooth edges.

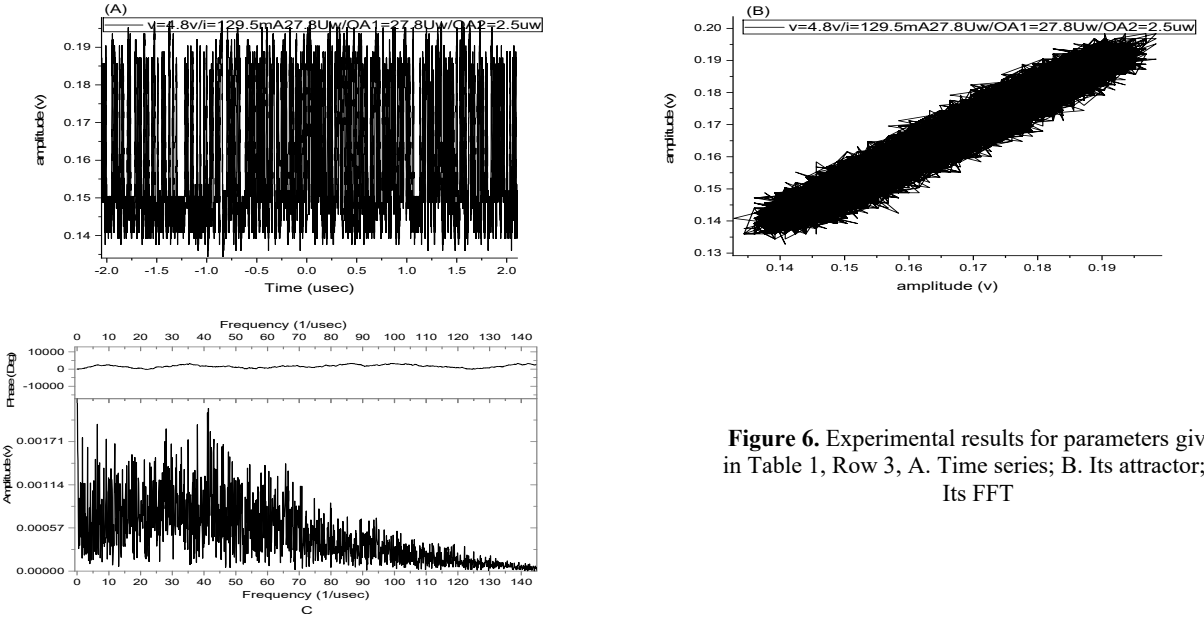

Figure 6. Experimental results for parameters given in Table 1, Row 3, A. Time series; B. Its attractor; C. Its FFT

Slightly deviating from the feedback filtering attenuation, precisely to a new ratio of 11.12 percent between branch one and branch two, the results given in Figure 7 recorded another variation in the observed spectrum, such that the attractor deviated from its original smooth edges to several distinguishable modes in the higher amplitude region. While the frequency spectrum is shrinking to only 13 MHz, the signal shape is now far away from its original Gaussian shape with a slightly higher amplitude.

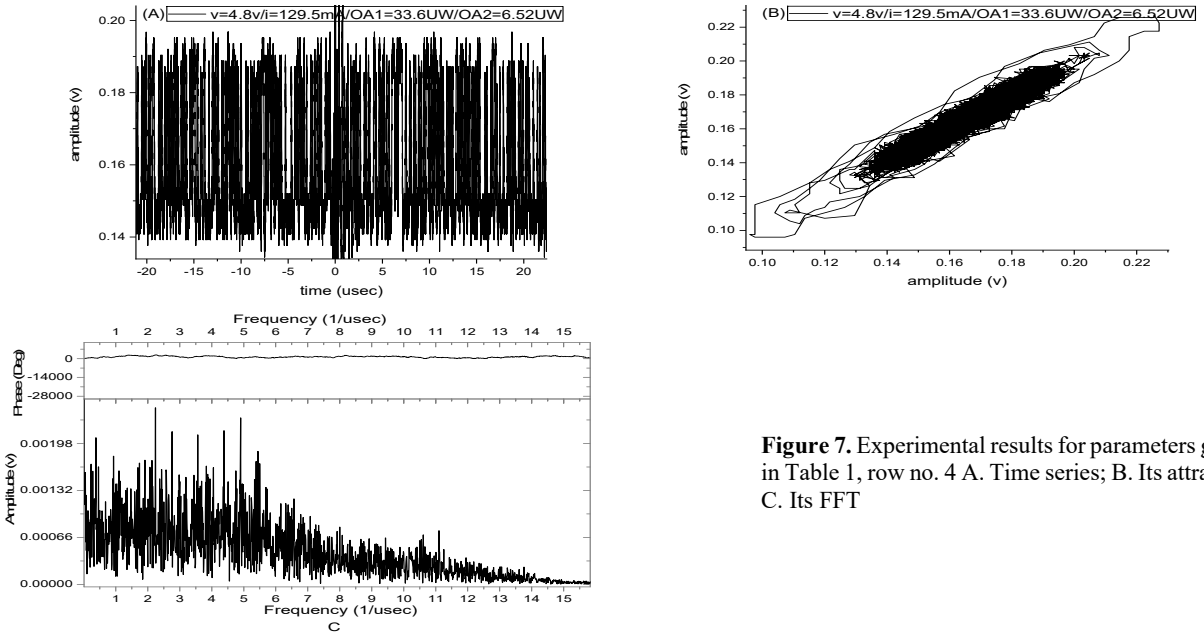

Figure 7. Experimental results for parameters given in Table 1, row no. 4 A. Time series; B. Its attractor; C. Its FFT

Decreasing the difference between the two feedback branches, the ratio is now 3.5 percent between branch one and branch two, the time series is still chaotic, the phase space repeated its smooth edges, and the frequency spectrum kept its chaotic broadening with a slight difference in overall shape, as shown in Figure 8.

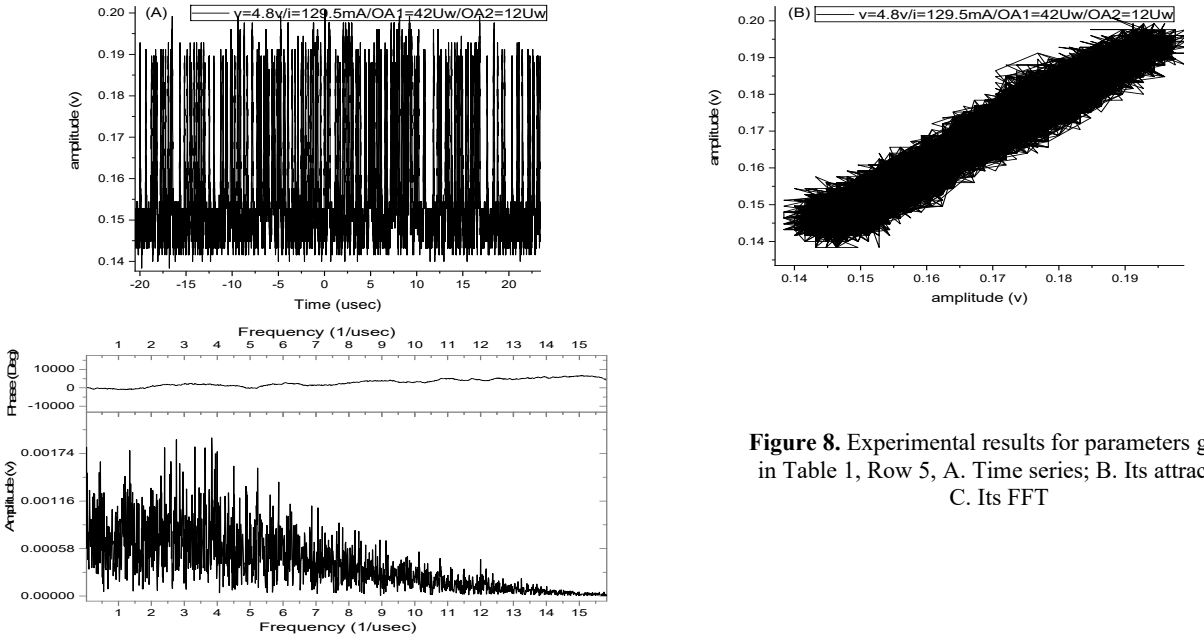

Figure 8. Experimental results for parameters given in Table 1, Row 5, A. Time series; B. Its attractor; C. Its FFT

A few fundamental presumptions form the foundation of theoretical neurophysiology. The nervous system is made up of a network of neurons, each with an axon and a soma. The axon of one neuron and the soma of another are always connected by adjunctions, or synapses. Refs. [5] and [3] reported that a neuron always has a threshold that stimulation must surpass in order to start an impulse. This level can be considered a starting point for the chaotic dynamics emission from the LD. This level of edge-emitted lasers was measured corresponding to the free-running laser threshold, i.e., applied bias voltage into the device with respect to that threshold. As it is mentioned inside all previewed results, the bias voltage selection is located at a faraway value from the laser threshold. The judgment in our selection of that value is the chaotic release that we need to be near from our application requirements. Figure 9 gives the resulted dynamics measurements, which have a ratio of 1.7 percent between branch one and branch two.

Generalization can be done when a layered feedforwarded as a neural network, that is by connecting Adalines to one another. The objective is to select the network's weights in order to obtain the appropriate input/output relationship. The network gets trained during this procedure. When the weights are kept constant, the output vector of the network can be said to be memoryless because it is independent of previous inputs and solely depends on the current input vector. As reported in Table 1 many weights are experimented to make the best selection from them.

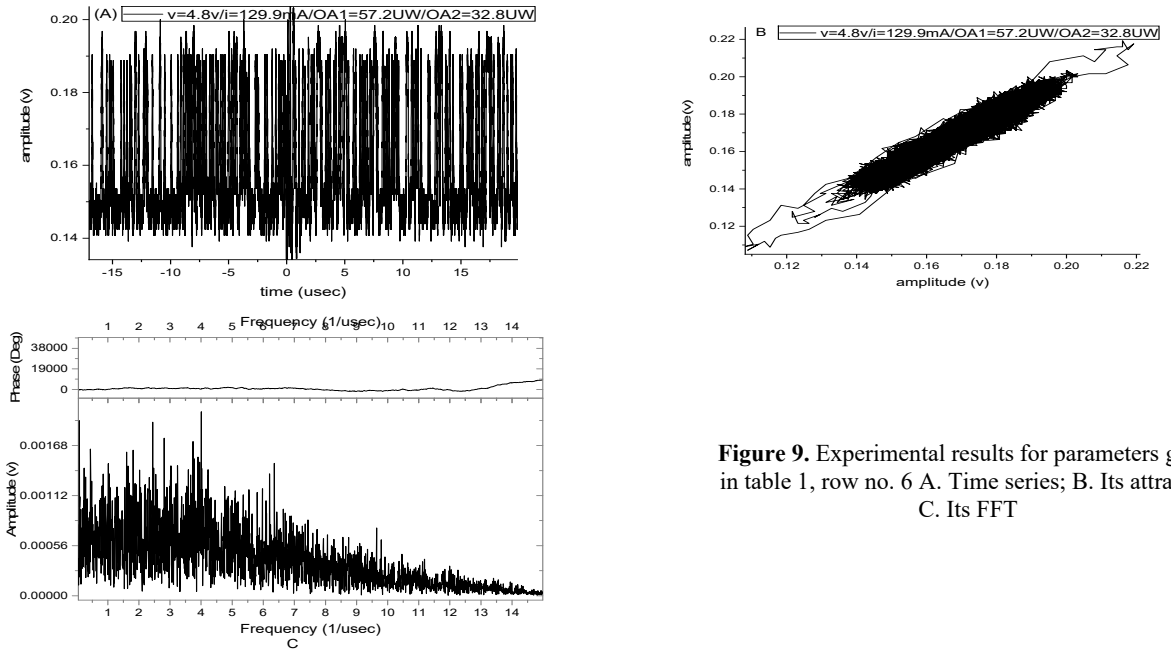

Figure 9. Experimental results for parameters given in table 1, row no. 6 A. Time series; B. Its attractor; C. Its FFT

With 1.13 percent between branch one and two, Figure 10, the lasing chaotic spectrum disappeared; instead, destructive behavior of the signal was observed, indicating only noise emission. The role of FBG is to give the operation loop a gate, i.e., in this operation level, the signal becomes larger in its wavelength spectrum spread, and if all included wavelets have a larger Bragg wavelength, they are blocked from transmission. Refs. [23] and [24] reported that the FBG gate can play the role of a wide or narrow filter to the incident signal according to the relation between the incident wavelength spectrum and its entire Bragg wavelength.

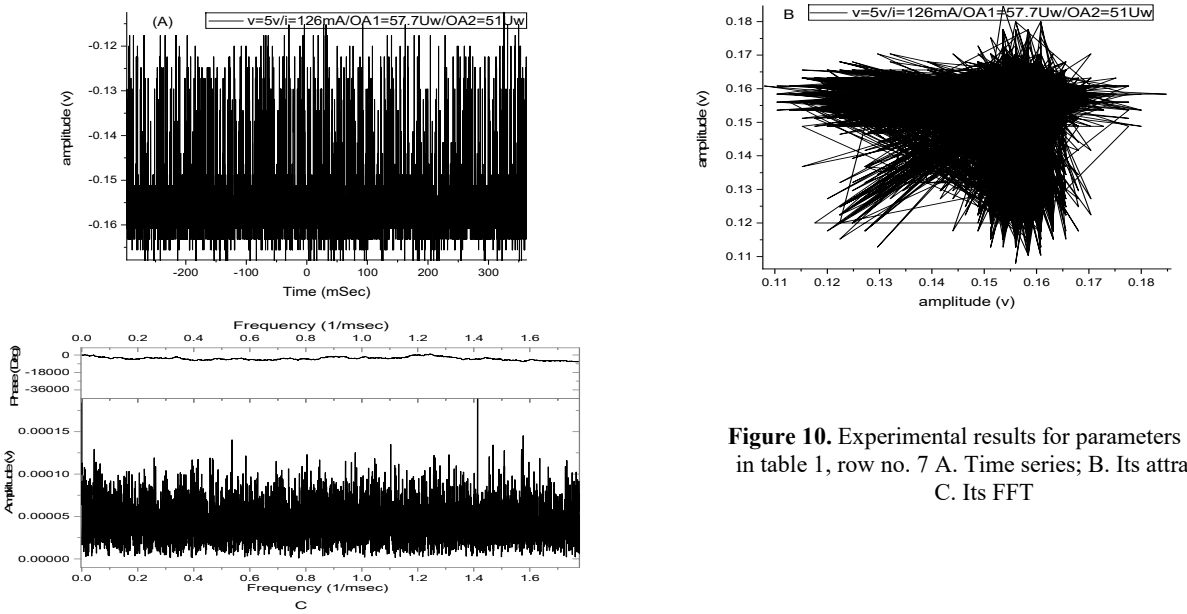

Figure 10. Experimental results for parameters given in table 1, row no. 7 A. Time series; B. Its attractor; C. Its FFT

Working with a 0.425 ratio between branches one and two (Figure 11), the maximum amplitudes return to be apparent, indicating matching between the incident signal and the Bragg wavelength for the filter. Around 7 MHz of chaotic signal width is observed with a circular attractor that includes several outer modes. When the output is modest due to laser medium nonlinearity, the Adaline filter behaves like a linear filter, but as the output amplitude increases, it saturates to +1 or -1. It should be noticed that the default setting for one of Adaline's inputs is +1. This gives the Adaline a technique to provide the weighted sum with a constant bias.

Working with an increased ratio of 0.895 in Figure 12, between branch one and two, the attractor is divided into three regions with a single mode outside of them. The frequency spectrum is extended to about 8 GHz, indicating large filter operation. Figures 13 and 14 give results for ratios of 7.925 and 0.548, respectively, between branches one and two. Both of these two measurements mention the existence of transmission, but with a slightly higher transmission ratio that appears as a broadening in the two observed spectra.

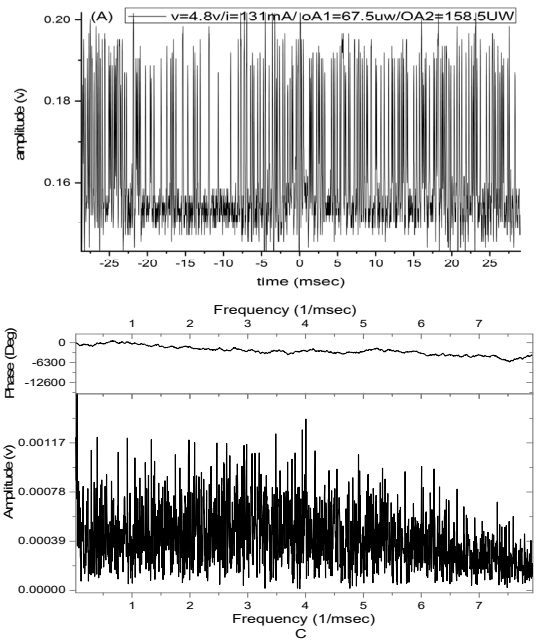

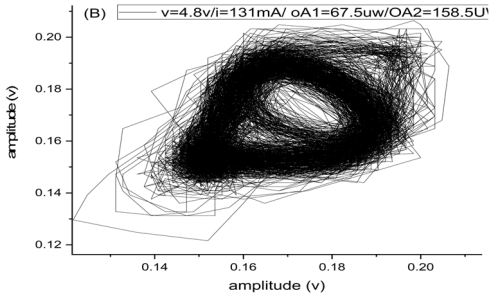

Figure 11. Experimental results for parameters given in table 1, row no. 8 A. Time series; B. Its attractor; C. Its FFT

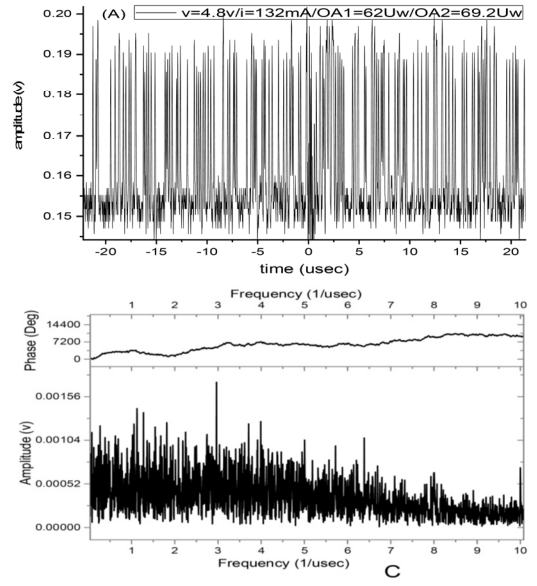

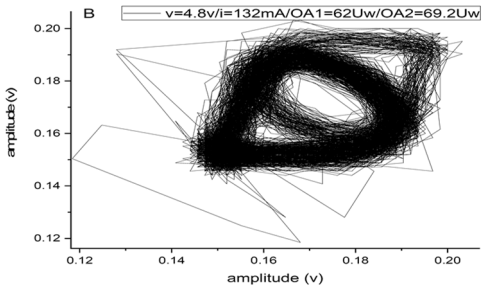

Figure 12. Experimental results for parameters given in table 1, row 9. A. Time series; B. Its attractor; C. Its FFT

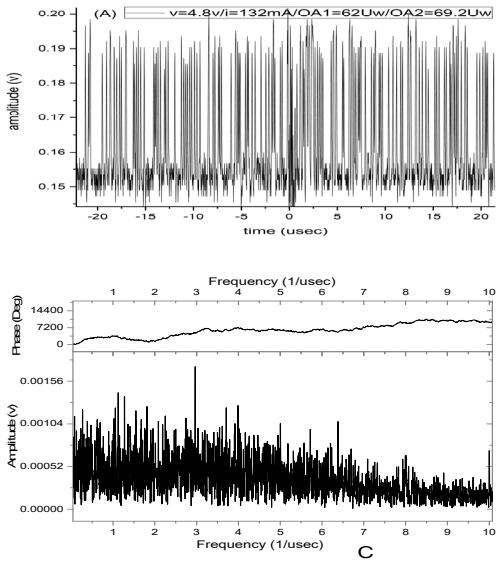

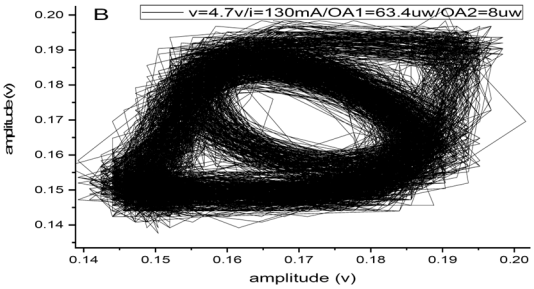

Figure 13. Experimental results for parameters given in table 1, row no. 10 A. Time series; B. Its attractor; C. Its FFT

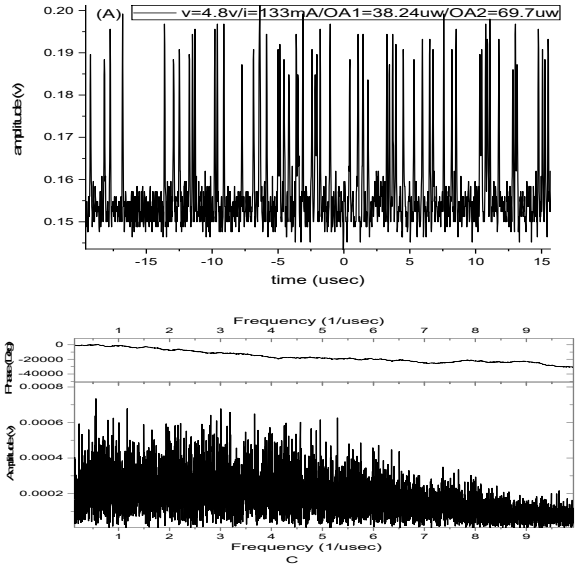

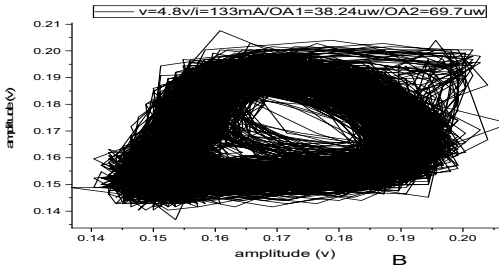

Figure 14. Experimental results for parameters given in Table 1, Row 11, A. Time series; B. Its attractor; C. Its FFT

CONCLUSIONS

The input layer experiment is satisfied, and through experimentation, the all-electrical architecture was contrasted with the hybrid and all-optical approaches. The all-optical technique is comparable to the hybrid strategy in terms of energy efficiency, outperforming the all-electrical approach. The hybrid architecture takes up much less space than the all-optical version because it only uses narrow filters. The feed-back versus feed-forward is tested as a step for the network's construction by combining an increased number of these layers. A ratio of 11.12 percent between branches one and two in this experiment gives a better contribution to the output chaotic signal compared with all measured values.

Acknowledgments

We gratefully acknowledge the assistance of Al-Mustansiriyah University and the University of Al-Nahrain in Baghdad, Iraq.

ORCID IDs

Dhuha Raad Madhloom, https://orcid.org/0009-0008-7053-2754; **Ayser A. Hemed,** https://orcid.org/0000-0003-0319-1650, **Suha Musa Khorsheed,** https://orcid.org/0000-0002-9544-3677

REFERENCES

[1] X. Sui, Q. Wu, L. Jia, Q. Chen, and G. Gu, "A Review of Optical Neural Networks," IEEE Access, **8**, 70773-70783 (2020). https://doi.org/10.1109/ACCESS.2020.2987333

[2] N. Kadakia, "Optimal control methods for nonlinear parameter estimation in biophysical neuron models," bioRxiv preprint, 2022. https://doi.org/10.1101/2022.01.11.475951

[3] F.P. Sunny, E. Taheri, M. Nikdast, and S. Pasricha, "A Survey on Silicon Photonics for Deep Learning,"ACM Journal on Emerging Technologies in Computing Systems, **17**(4), 1-57 (2021). https://doi.org/10.1145/3459009

[4] E. Cohen, D. Malka, A. Shemer, A. Shahmoon, Z. Zalevsky, and M. London, "Neural networks within multi-core optic fibers," Scientific Reports, **6**, 1-14 (2016). https://doi.org/10.1038/srep29080

[5] D.H. Nguyen, and B. Widrow, "Neural Networks for Self-Learning Control Systems," IEEE Control Systems Magazine, **10**(3), 18-23 (1990). https://doi.org/10.1109/37.55119

[6] W.S. Mcculloch, and W. Pits, "A logical calculus of the ideas immanent in nervous activity," Bulletin of Mathematical Biophysics, **5,** 115-133 (1943). https://doi.org/10.1007/BF02478259

[7] R.F. Thompson, "The neurobiology of learning and memory," in: *Clinical neuropsychology and brain function: Research, measurement, and practice,* edited by T. Boll, and B.K. Bryant (American Psychological Association, Vashington, 1988). pp. 61-83, https://doi.org/10.1037/10063-002

[8] T. Staff, "Deep learning - 10 breakthrough technologies 2013," MIT Technology Review, 2013.

[9] F.-C.F. Tsai, C.J. O'Brien, N.S. Petrović, and A.D. Rakić, "Analysis of optical channel cross talk for free-space optical interconnects in the presence of higher-order transverse modes," Applied Optics, **44**(30), 6380-6387 (2005). https://doi.org/10.1364/AO.44.006380

[10] R. Clark, L. Fuller, J. Platt, and H.D.I. Abarbanel, "Reduced-Dimension, Biophysical Neuron Models Constructed From Observed Data," Neural Comput. **34**(7), 1545-1587 (2022). https://doi.org/10.1162/neco_a_01515.

A. Uchida, *Optical Communication with Chaotic Lasers: Applications of Nonlinear Dynamics and Synchronization*, (Wiley-VCH Verlag GmbH & Co., KGaA, 2012).

[11] M. Ahmed, A. Bakry, and F. Koyama, "Application of Strong Optical Feedback to Enhance the Modulation Bandwidth of Semiconductor Lasers to the Millimeter-Wave Band," International J. Physical and Mathematical Science, **9**(1), 17-22 (2015). https://doi.org/10.5281/zenodo.1337753

[12] D.R. Hjelme, and A. Mickelson, "On the theory of external cavity operated single-mode semiconductor lasers," IEEE Journal of Quantum Electronics, **23**(6), 1000-1004 (1987). https://doi.org/10.1109/JQE.1987.1073460

[13] G.P. Agrawal, "Effect of gain nonlinearities on period doubling and chaos in directly modulated semiconductor lasers," Applied Physics Letters, **49**(16), 1013-1015 (1986), https://doi.org/10.1063/1.97456
[14] V. Bindu, and V.M. Nandakumaran, "Chaotic encryption using long-wavelength directly modulated semiconductor lasers," Journal of Optics A: Pure and Applied Optics, **4**(2), 115-119 (2002). https://doi.org/10.1088/1464-4258/4/2/301
[15] G.P. Agrawal, and N.K. Dutta, *Semiconductor Lasers*, Second Edition, (Dordrecht: Kluwer Academic Publishers, 1993).
[16] F.-Y. Lin, and J.-M. Liu, "Nonlinear Dyanmic of Semiconductor Laser with Delayed Optoelectronic Feedback," IEEE Journal of Quantum Electronics, **39**(4), 562-568 (2003), https://doi.org/10.1109/JQE.2003.809338
[17] G. Giacomelli, M. Calzavara, and F.T. Arecchi, "Instabilities in a semiconductor laser with delayed optoelectronic feedback," Optics Communications, **74**(1-2), 97-101 (1989). https://doi.org/10.1016/0030-4018(89)90498-7
[18] H. Erzgraber, B. Krauskopf, D. Lenstra, A. Fischer and G. Vemuri, , *Phys Rev E Stat Nonlin Soft Matter Phys,* **76**, no. 2, (2007), https://doi.org/10.1103/PhysRevE.76.026212
[19] A. Hemed, Ph.D. dissertation, University of Baghdad-Iraq, 2011.
[20] V.L. Kalyani, and V. Sharma, "Different types of optical filter and their application," Journal of Management Engineering and Information Technology, **3**(3), 12-17 (2016).
[21] A.M. Suhail, B.T. Chead, H.J. Kbashi, and A.A. Hemed, "Studying the effect of variant optoelectronic feedback on chaos generation," Atti della Fondazione Giorgio Ronchi, Chaos, Anno, **LXV**(2), 147-154 (2010).
[22] Z.R. Ghayib, Ph.D. dissertation, College of Education at Mustansiriyah University, 2022.
[23] A. Hemed, and Z.R. Gaiab, in: *2022 International Conference on Computer Science and Software Engineering CSASE*, Duhok, Kurdistan Region – Iraq, 2022. https://doi.org/10.1109/csase51777.2022.9759612
[24] G. Fennessy, and Y. Vorobeychik, "Optical Neural Networks," https://doi.org/10.48550/arXiv.1805.06082

ЕКСПЕРИМЕНТАЛЬНЕ МОДЕЛЮВАННЯ ДВОХ ОПТИЧНО ФІЛЬТРОВАНИХ МОДУЛЯЦІЙНИХ ВАГ В ЛАЗЕРНОМУ ДІОДІ ЯК ШАРІ З САМОНАВЧАННЯМ

Дхуха Раад Мадлум[a], Айсер А. Хемед[b], Суха Муса Хоршід[a]
[a]*Факультет фізики, Науковий коледж, Університет Аль-Нахрейн, Багдад, Ірак*
[b]*Факультет фізики, Педагогічний коледж, Університет Мустансірія, Багдад, Ірак*

У цьому дослідженні експериментально досліджено відгук нелінійного лазерного середовища. У дослідженні гібридна версія вхідного шару, який розмножується оптично та накопичує електрично, порівнюється з повністю оптичною версією, яка розмножується та накопичує оптично. Це середовище зазнає двох різних шляхів оптично відфільтрованого та ослабленого зворотного зв'язку. У такій системі зміна ваги зворотного зв'язку в одному з них перевіряється відповідно до другого. Спостереження за частотними спектрами проводяться для моделювання результуючої реакції з вхідним рівнем для нейронної мережі на основі хаотичних несучих. Хаотичне лазерне випромінювання спостерігалося як функція кількох керуючих параметрів, якими є напруга зміщення постійного струму, оптичне загасання в гілці та інтенсивність зворотного зв'язку на основі фільтрації за допомогою волоконної ґратки Брегга. Це правило навчання є лінійним у різниці між кожним входом і виходом нейрона. Це правило посилення/затримки. Пороги регулюються таким чином, що вихід нейрона або підштовхується в тому ж напрямку, що і вхід (посилення), або в протилежному напрямку (гальмування).

Ключові слова: *машинне навчання; нейронна мережа; хаотична модуляція; лазерний діод*